Overexpression/enhanced kinase activity of BCR/ABL and altered expression of Notch1 induced acute leukemia in p210BCR/ABL transgenic mice

Toshiyuki Mizuno[1,2], Norimasa Yamasaki[1], Kazuko Miyazaki[1], Tatsuya Tazaki[1], Richard Koller[3], Hideaki Oda[4], Zen-ichiro Honda[5], Mitsuo Ochi[2], Linda Wolff[3], and *Hiroaki Honda[1]

[1]Department of Developmental Biology, Research Institute of Radiation Biology and Medicine, Hiroshima University, 1-2-3 Kasumi, Minami-ku, Hiroshima 734-8553, Japan. [2]Department of Orthopedic Surgery, Hiroshima University School of Medicine, Hiroshima University, 1-2-3 Kasumi, Minami-ku, Hiroshima 734-8553, Japan. [3]Leukemogenesis Section, Laboratory of Cellular Oncology, National Cancer Institute, NIH, 9000 Rockville Pike, Bethesda, MD 20892-4263, USA. [4]Department of Pathology, Tokyo Women's Medical University, 8-1 Kawada-cho, Shinjuku-ku, Tokyo 162-8666, Japan. [5]Department of Allergy and Rheumatology, Faculty of Medicine, Graduate School of Medicine, University of Tokyo, 7-3-1 Hongo, Bunkyo-ku, Tokyo 113-8655, Japan.

*Corresponding author: Hiroaki Honda, Department of Developmental Biology, Research Institute of Radiation Biology and Medicine, Hiroshima University, 1-2-3 Kasumi, Minami-ku, Hiroshima 734-8553, Japan.
Phone: +82-257-5819, Fax: +82-256-7107, e-mail: hhonda@hiroshima-u.ac.jp

Running title: p210BCR/ABL and Notch1 expression in CML BC

Key words: Chronic myelogenous leukemia (CML), blast crisis (BC), transgenic mice (Tg), p210BCR/ABL, Notch1

Abstract words: 204, Text words: 6317

Abstract

Chronic myelogenous leukemia (CML) is a hematopoietic disorder, which begins as indolent chronic phase but inevitably progresses to fatal blast crisis. p210BCR/ABL, a constitutively active tyrosine kinase, is responsible for disease initiation but molecular mechanism(s) underlying disease evolution remains largely unknown. To explore this process, we employed retroviral insertional mutagenesis to CML-exhibiting *p210BCR/ABL* transgenic mice (Tg). Virus infection induced acute lymphoblastic leukemia (ALL) in *p210BCR/ABL* Tg with a higher frequency and in a shorter latency than wild-type littermates, and inverse PCR detected two retrovirus common integration sites (CISs) in *p210BCR/ABL* Tg tumors. Interestingly, one CIS was the transgene itself, where retrovirus integrations induced upregulation of p210BCR/ABL and production of truncated BCR/ABL with an enhanced kinase activity. Another CIS was *Notch1* gene, where retrovirus integrations resulted in overexpression of Notch1 and generation of Notch1 lacking the C-terminal region (Notch1ΔC) associated with stable expression of its activated product, C-terminus-truncated Notch intracellular domain (NICDΔC). In addition, generation of Tg for both *p210BCR/ABL* and *Notch1ΔC* developed ALL in a shortened period with Stat5 activation, demonstrating the cooperative oncogenicity of Notch1ΔC/NICDΔC with p210BCR/ABL involving Stat5-mediated pathway. These results demonstrated that overexpression/enhanced kinase activity of BCR/ABL and altered expression of Notch1 induce acute leukemia in a transgenic model for CML.

Introduction

Chronic myelogenous leukemia (CML) is a clonal disorder originated from multipotential hematopoietic stem cells, which shows excessive proliferation of differentiated myeloid cells (Deininger *et al.*, 2000; Ren, 2005). The clinical course of the disease is characterized by its hematologically and temporally distinct stages (Deininger *et al.*, 2000; Ren, 2005). In the initial stage, chronic phase (CP), the disease is indolent and the leukemic cells retain an ability to differentiate into mature myeloid cells. After several years' duration of the chronic phase, however, the disease inevitably accelerates and ultimately progresses to the terminal fatal stage, blast crisis (BC), which involves rapid expansion of differentiation-arrested blast cells.

Cytogenetically, CML CP is associated with the Ph chromosome, a shortened chromosome 22, resulting from a reciprocal chromosomal translocation between chromosome 9 and 22 (t(9;22)(q34;q11)) (Rowley, 1973). This fuses 5' portion of *BCR* gene to 3' portion of *ABL* proto-oncogene, thereby creating *BCR/ABL* chimeric mRNA encoding 210KD hybrid protein (p210BCR/ABL). p210BCR/ABL possesses a constitutively active kinase activity, which is believed to initiate CP. In contrast, mechanism(s) responsible for transition from CP to BC remains poorly understood, although the appearance of nonrandom chromosomal abnormalities in BC strongly suggests that additional events would account for disease progression (Deininger *et al.*, 2000; Ren, 2005).

To understand the complex clinical course of human CML, it is necessary to develop animal models. Major attempts have been focused on bone marrow transplantation (BMT) experiments. Transplantation of BM cells infected with *p210BCR/ABL*-expressing retroviruses into irradiated mice induced rapid proliferation of differentiated myeloid cells (Pear *et al.*, 1998; Zhang & Ren, 1998; Li *et al.*, 1999). On the other hand, transgenic mice (Tg) expressing *p210BCR/ABL* under various promoters also provided useful models (Honda *et al.*, 1995; Voncken *et al.*, 1995;

Honda *et al.*, 1998; Huettner *et al.*, 2000; Huettner *et al.*, 2003; Koschmieder *et al.*, 2005). We generated Tg expressing *p210BCR/ABL* under the control of mouse *TEC* promoter (Honda *et al.*, 1997) and demonstrated that the transgenic progeny reproducibly exhibited a myeloproliferative disorder closely resembling to human CML (Honda *et al.*, 1998). We then crossed *p210BCR/ABL* Tg with *p53* heterozygous mice and demonstrated that acquired and preferential loss of *p53* in *p210BCR/ABL*-expressing hematopoietic cells induced BC (Honda *et al.*, 2000). In addition, we crossed *p210BCR/ABL* Tg with *Dok-1*/*Dok-2* knockout mice and showed that the absence of Dok-1 and Dok-2 accelerated disease phenotype and caused BC, demonstrating that Dok-1 and Dok-2 function as tumor suppressors (Niki *et al.*, 2004). Based on these results, our *p210BCR/ABL* Tg can be regarded as a useful model for investigating molecular mechanism(s) underlying the progression from CML CP to BC.

In this report, to identify gene(s) whose altered expression contributes to disease evolution of CML, we employed retroviral insertional mutagenesis to the *p210BCR/ABL* Tg, by directly injecting Moloney murine leukemia virus (MMLV) (Jonkers & Berns, 1996) and its derivative, MOL4070LTR (Wolff *et al.*, 2003b), into newborn mice.

Results

MMLV induced T-cell ALL in *p210BCR/ABL* Tg with a higher incidence and in a shorter period than wild-type littermates (WT)

MMLV-injection induced acute leukemia in both *p210BCR/ABL* Tg and WT, but the disease frequency and latency were significantly different between the two groups. As shown in Fig. 1A, in contrast that WT injected with MMLV (WT/MMLV) developed acute leukemia after 5 months after birth (dotted line), *p210BCR/ABL* Tg injected with MMLV (p210BCR/ABL/MMLV) began to develop acute leukemia at as early as 2 months of age and all Tg died within 4 months of age (thick line). All the leukemic mice exhibited massive thymoma and splenomegaly, and pathological analysis showed proliferation of blast cells in the peripheral blood, thymus, spleen, and other tissues. Since the leukemic cells exclusively expressed a T-cell antigen, they were diagnosed as T-cell ALL (T-ALL). The representative results of pathological and flow cytometric analyses of a T-ALL mouse (MMLV-2) are shown in Fig. 2A (left panel) and Fig. 2B (upper panel), respectively, and characteristics of p210BCR/ABL/MMLV leukemic mice are summarized in Table 1.

MOL4070 induced T-cell and B-cell ALL in p210BCR/ABL Tg while no disease was observed in WT

MOL4070LTR injection induced acute leukemia in 6 out of 11 *p210BCR/ABL* Tg (p210BCR/ABL/MOL4070), while no disease was observed in virus-injected WT (Fig. 1B). Among the diseased mice, 3 mice (MOL4070-3, -4, and -6) showed thymic enlargement as observed in p210BCR/ABL/MMLV, whereas other 3 mice (MOL4070-1, -2, and -5) exhibited different phenotypes. MOL4070-1 developed a tumor on the right shoulder at 3 months of age. Since the tumor enlarged and the peripheral blood smear showed proliferation of blast cells, the mouse was diagnosed as acute leukemia with blastoma. The other two mice (MOL4070-2 and -5) exhibited multiple LN swellings

and splenomegaly but no thymic enlargement was evident.

Blast cells of the former 3 mice (MOL4070-3, -4, and -6) were positive for a T-cell antigen and were diagnosed as T-ALL, whereas those of the latter 3 mice (MOL4070-1, -2, and -5) were positive for a B-cell antigen and were considered to develop B-cell ALL (B-ALL). The representative results of pathological and flow cytometric analyses of a B-ALL mouse (MOL4070-1) are shown in Fig. 2A (right panel) and 2B (lower panel), respectively, and characteristics of p210BCR/ABL/MOL4070 leukemic mice are summarized in Table 2.

Identification of the transgene as a retrovirus common integration site in B-cell leukemias

The results that retrovirus-injected p210BCR/ABL developed acute leukemia with higher morbidity and mortality than virus-injected WT (Fig. 1A and 1B) indicated that alteration(s) in gene expression by retroviral integration cooperated with p210BCR/ABL and induced ALL. To identify virus-integrated genes, DNAs extracted from leukemic tissues were subjected to inverse PCR (iPCR).

We first tried to identify retrovirus common integration sites (CISs) in B-ALL cases, since in human CML BC, B-cell crisis is more frequently observed than T-cell one (Pane *et al.*, 2002). Among iPCR fragments obtained from B-cell leukemias (MOL4070-1, -2, and -5, see supplemental Table 2), we found one interesting PCR product in MOL4070-1, in which a retrovirus integrated in the promoter region of mouse *TEC* gene but sequencing of whole PCR product revealed that the sequences were interrupted and followed by human *BCR/ABL* cDNA. Since this exactly corresponds to the structure of the *p210BCR/ABL* transgene (Honda *et al.*, 1998), the integration site was disclosed to be not in the endogenous *TEC* promoter but in the promoter region of the transgene. In addition, an integration site was found in the coding region of *ABL* gene in MOL4070-2, but curiously, the sequences had only an

~80% homology to mouse *ABL* gene but completely matched human *ABL* gene, indicating that the integration occurred not in the endogenous *ABL* gene but in the *ABL*-coding region of the transgene. Based on these findings, the transgene was identified as a CIS, where integrations occurred in the promoter and in the *ABL*-coding regions. In the latter case, the retrovirus insertion created a new stop codon at nucleotide 5116, which would produce truncated BCR/ABL. The schematic model of the integration sites and resultant protein products in these mice are shown in Fig. 3A.

Overexpression of p210BCR/ABL and expression of truncated BCR/ABL with an enhanced kinase activity

To examine cells with these integration sites to be a major part in the tumors, Southern blot was performed using transgene-derived fragments adjacent to the integration sites. DNA extracted from a virus-non-infected *p210BCR/ABL* transgenic spleen was used as a control. As shown in Fig. 3B, rearranged bands were detected in both cases (indicated by an arrowheads), demonstrating that these integration sites were the major integration sites and that the tumors were clonal in origin.

To investigate whether these integrations altered the expression and/or the kinase activity of p210BCR/ABL, we performed Northern blot and an *in vitro* kinase assay using RNAs and proteins extracted from the tumors. Virus-not-infected *p210BCR/ABL* transgenic spleen and tumors of MOL4070-3~MOL4070-5, in which retrovirus was not integrated in the transgene, were used as controls. The results are shown in Fig. 3C and 3D.

It is not surprising that expression of *p210BCR/ABL* message or phosphorylation of p210BCR/ABL protein was not detected in the control *p210BCR/ABL* transgenic spleen (Fig. 3C ad 3D), since our previous data demonstrated that the basal transgene expression was quite low, probably due to the nature of the promoter used (Honda *et al.*, 1998). Enhanced expression of *p210BCR/ABL* mRNA and phosphorylation of its

protein product were observed in MOL4070-1 (indicated by an arrowhead in Fig. 3C and 3D). In addition, although no upregulation of the transgene-derived mRNA was apparent, a ~160KDa phosphorylated band corresponding to the molecular weight of the truncated BCR/ABL was evident in MOL4070-2 (indicated by an arrow in Fig. 3D). These results demonstrated that retrovirus integrations in MOL4070-1 and MOL4070-2 induced overexpression of p210BCR/ABL and truncated BCR/ABL with an enhanced kinase activity, respectively.

Identification of *Notch1* gene as a retrovirus common integration site in T-cell leukemias

Among genes isolated by iPCR in T-ALL cases developed in *p210BCR/ABL* Tg (MMLV1~10 and MOL4070-3, -4, and -6, listed on supplemental Table 1 and 2), we identified another CIS, *Notch1* gene, that encodes a transmembrane protein involved in cellular signaling (Ellisen *et al.*, 1991). In two *Notch1*-integrated cases, one integration was found in the second intron (MMLV-1), while the other occurred in the coding region of the last exon (MMLV-6), which created a new stop codon at nucleotide 7114 and would produce a truncated protein lacking the C-terminal domain. The schematic model of the integration sites and protein products in the two *Notch1*-inserted cases is shown in Fig. 4A.

Overexpression of Notch1 and expression of Notch1 lacking the C-terminal region (Notch1ΔC) with its activated product, C-terminus-truncated Notch1 intracellular domain (NICDΔC)

To investigate cells with these *Notch1*-integration sites to be a major population in the tumors, Southern blot was performed using genomic fragments adjacent to the integration sites. As shown in Fig. 4B, in both MMLV-1 and MMLV-6, a rearranged band was detected (indicated as arrowheads), demonstrating these sites to be major

integration sites.

We next investigated possible alteration in *Notch1* expression in these *Notch1*-inserted leukemias by Northern blot using Notch1 cDNA and by Western blot using an anti-Notch1 antibody, mN1A. Virus-non-injected transgenic thymus and thymomas of MMLV-3~MMLV-5, in which retrovirus was not integrated in *Notch1* gene, were used as controls. As shown in Fig. 4C and 4D (upper panels), at both mRNA and protein levels, overexpression of Notch1 was observed in MMLV-1 (indicated by an arrowhead) and expression of Notch1 lacking C-terminal region (Notch1ΔC) was detected in MMLV-6 (indicated by an arrow). In addition, in the Western blot, since the mN1A antibody recognizes not only full-length Notch1 (>200 KDa) but also cleaved Notch1 (~120 KDa), the expressional changes of Notch1 in MMLV-1 and MMLV-6 were found to be associated with enhanced expression of Notch1 transmembrane subunit (NTM), the product after S1 cleavage, and stable expression of C-terminus-deleted NTM (NTMΔC), respectively (indicated by a white triangle and by an arrow in Fig. 4D). To investigate whether the altered expression of Notch1/NTM and Notch1ΔC/NTMΔC affected the expression of Notch1 intracellular domain (NICD), the active form of Notch1 after S3 cleavage, the same samples were blotted with Val1477 antibody that specifically recognizes NICD. As shown in the lower panel of Fig. 4D, expression of NICDΔC was observed in MMLV-6, whereas no apparent expression of NICD was detected in other samples including MMLV-1. These results indicated that the retrovirus insertion in MMLV-1 induced overexpression of Notch1 and NTM, whereas that in MMLV-6 resulted in expression of Notch1ΔC, which led to stable expression of NTMΔC and NICDΔC.

Double Tg for *p210BCR/ABL* and *Notch1ΔC* developed T-ALL with Stat5 activation

We finally examined whether Notch1ΔC/NICDΔC cooperates with

p210BCR/ABL and induces acute leukemia *in vivo*. To this aim, we generated *Notch1ΔC* Tg, crossed them with *p210BCR/ABL* Tg, and created double Tg for both *p210BCR/ABL* and *Notch1ΔC*. Since MMLV-6 developed T-ALL, the *lck* promoter, which drives transgene expression in thymocytes (Abraham *et al.*, 1991), was chosen as a regulatory element and to facilitate detection of *Notch1ΔC*, an *Flag-HA* (*FH*) tag was added to the 5' portion of *Notch1ΔC* cDNA (Fig. 5A).

Among several transgenic lines produced, a line with high *Notch1ΔC* expression, screened by anti-FH and anti-Notch1 Western blots (data not shown), was used for crossing with *p210BCR/ABL* Tg. The survival curves of the offspring are shown in Fig. 5B. During about 6 months' observation, a half of double Tg developed massive thymic enlargement showing expression of a T-cell antigen (data not shown), while none of *p210BCR/ABL* or *lck/Notch1ΔC* Tg alone developed hematological disease. To examine that tumors in double transgenic mice expressed Notch1ΔC and p210BCR/ABL proteins, cell lysates extracted from control transgenic thymuses (*p210BCR/ABL* Tg (C1) and *lck/Notch1ΔC* Tg (C2)) and tumors of double transgenic mice (No.1~4) were blotted with anti-Notch1 and anti-ABL antibodies. As shown in upper and middle panels of Fig. 5C, all the tumors in addition to C2 expressed Notch1ΔC/NTMΔC by anti-mN1A Western blot, and expression of NICDΔC in these samples was confirmed by anti-Val1477 Western blot. In addition, stable expression of p210BCR/ABL in the tumors was detected by anti-ABL Western blot (lower panel of Fig. 5C). These results indicated the cooperative role of Notch1ΔC/NICDΔC and p210BCR/ABL in tumor development. We further investigated alteration in tyrosine-phosphorylation in the tumors, by using an anti-phosphotyrosine (P-Tyr) antibody (upper panel of Fig. 5D). Two major tyrosine-phosphorylated bands were detected in the tumors (shown by an arrow and an arrowhead). The upper band (~200KDa) was identified as tyrosine-phosphorylated p210BCR/ABL, while lower band (~97KDa) corresponds to molecular weight of Stat5, a signal transducer involved in p210BCR/ABL-mediated

pathway. To examine whether this band was Stat5, we immunoprecipitated proteins with an anti-Stat5 antibody and blotted immunoprecipitants with the same antibody or with an anti-PTyr antibody. The results showed the tyrosine phosphorylation of Stat5, demonstrating the activation of Stat5 in the tumors (Fig. 5D, lower panels).

Discussion

Carcinogenesis results from accumulation of sequential genetic changes. In this respect, CML is an appropriate disease model in which generation of p210BCR/ABL initiates CP and subsequent genetic event(s) progresses the disease to BC. To identify gene(s) responsible for disease evolution, *p210BCR/ABL* Tg were subjected to retrovirus insertional mutagenesis, the method that has successfully identified cooperative genes in gene-engineered mice (Jonkers & Berns, 1996; Mikkers & Berns, 2003; Nakamura, 2005). MMLV and its derivative, MOL4070LTR, were used in this study. MOL4070LTR was generated as a hybrid retrovirus by replacing a part of MMLV LTR with that of 4070A and it possesses a property to induce myeloid disease as well as lymphoid disease (Wolff *et al.*, 2003b). In our study, although no myeloid disease was observed, MOL4070LTR developed T- and B-ALL in contrast MMLV exclusively induced T-ALL, confirming that MOL4070LTR has a potential to induce expanded disease phenotypes as compared to the parental MMLV.

Pathological examination of the diseased mice showed that the bone marrow pictures already exhibited CML-like myeloid hyperplasia with maturation when they developed acute leukemia (a representative picture is shown in Supplemental Fig. 1). Therefore, it could be conceivable that CML already existed and alteration in gene expression induced by retrovirus integration accelerated the disease and consequently caused BC. To isolate genes responsible for disease evolution, we performed iPCR and identified two CISs; one for B-ALL and the other for T-ALL.

The CIS in 2 B-ALL cases was, interestingly, the transgene itself. The reason why the transgene was subjected to retrovirus attack remains unknown, but one possibility is that the transgene insertion in the genome might alter chromatin structure, which would consequently facilitate retrovirus integration. In these cases, overexpression of p210BCR/ABL and enhanced kinase activity of its truncated product were observed. These findings are very interesting, since double Ph, where p210BCR/ABL would be

more expressed than in CP, is one of the most frequently observed chromosomal abnormalities in CML BC (Calabretta & Perrotti, 2004) and our observation provides *in vivo* experimental evidence that acquired overexpression or enhanced kinase activity of p210BCR/ABL induces BC. In the BMT studies, *p210BCR/ABL* expression by retrovirus promoters would be much more abundant than that in our transgenic model, nevertheless, the recipient mice develop a rapid and fatal proliferation of differentiated myeloid cells but rarely exhibit an acute phenotype (Pear *et al.*, 1998; Zhang & Ren, 1998; Li *et al.*, 1999). These results lead us to the idea that initial *p210BCR/ABL* expression level affects aggressiveness and latency of CML CP, but high *p210BCR/ABL* expression alone is not sufficient to induce acute leukemia, and acquired overexpression/enhanced kinase activity of BCR/ABL is required for disease evolution.

In MOL4070-2, the mechanism of how C-terminal deletion of p210BCR/ABL rendered an enhanced kinase activity remains unknown. The structure of truncated BCR/ABL in MOL4070-2 very closely resembles to that of a BCR/ABL mutant isolated as possessing an enhanced kinase activity and a high transforming activity (Shore *et al.*, 1994). Thus, existence of a negative regulatory region in the deleted sequences or alteration in intramolecular/intermolecular interaction caused by the structural change might enhance BCR/ABL-induced kinase activity, as suggested previously (Shore *et al.*, 1994).

Another CIS was *Notch1* gene, originally cloned as a target gene in t(7;9)(q34;q34.3). Although this rearrangement accounts for only ~1% of human T-ALL (Ellisen *et al.*, 1991), recent studies demonstrated mutations in *Notch1* to be detected in a substantial population of T-ALL in human and also in mouse (Weng *et al.*, 2004; Lin *et al.*, 2006; O'Nei *et al.*, 2006). In both species, most of the mutations are detected in the HD (heterodimerization domain) and/or the PEST (polypeptide enriched in proline, glutamate, serine, and threonine) domain, as observed in case of MMLV-6 (Fig. 4A). The expressional changes in these domains are considered to contribute to

leukemogenesis by facilitating ligand-independent pathway activation and by increasing the half-life of transcriptionally active Notch1 intracellular domain (NICD) (Grabher *et al.*, 2006) and indeed, enhanced expression of NICDΔC was detected in MMLV-6 (Fig. 4D, lower panel). In case of MMLV-1, although we could not detect NICD by Western blot, it might be possible that the overexpression of Notch1/NTM would enhance expression of NICD. These results strongly suggest that activation of Notch1 would participate in the progression to acute phase of CML.

To confirm the contribution of Notch1ΔC/NICDΔC to CML-BC *in vivo*, we generated *lck/Notch1ΔC* Tg and crossed it with *p210BCR/ABL* Tg. Double Tg developed acute leukemia and expression of NICDΔC was detected in the tumors as well as in the thymus of a control *lck/Notch1ΔC* Tg (Fig. 5C), demonstrating the cooperative role of Notch1ΔC/NICDΔC with p210BCR/ABL in T-cell BC. Although T-cell crisis is rare in human CML BC, it would be intriguing to examine whether *Notch1* mutations are found in CML T-cell BC cases. Since an FH-tag was added to the N-terminus of Notch1ΔC to facilitate transgene expression, further studies will be required to clarify whether transgene-derived Notch1ΔC might be expressed as a membrane protein and activate downstream signaling by a ligand-dependent mechanism, or it might remain in the cytoplasm and exert its function by a ligand-independent mechanism (Bray, 2006; Ilagan & Kopan, 2007).

In addition, in the tumors of double Tg, we demonstrated that Stat5, a molecule involved in BCR/ABL-mediated signaling pathways (Shuai *et al.*, 1996; Scherr *et al.*, 2006; Ye *et al.*, 2006), was activated. Recent studies demonstrated that Notch and its effector, Hes, activate Stat families (Kamakura *et al.*, 2004; Monsalve *et al.*, 2006). Thus, it might be possible that Stat5 functions as a downstream target and its activation would play a role in ALL development in *p210BCR/ABL* and *Notch1ΔC* double Tg.

In addition to these two CISs, we also identified several genes that were shown to be major integration sites in the tumors by Southern blot, which included *IL21* receptor

(*IL21R*), *Ahi1*, *Cdk5rap2*, and *Lyt-2* for T-ALL, and *Evi3* for B-ALL (see supplemental Fig. 2 and supplemental Table 1 and 2). Although these results strongly suggest that altered expression of these genes might be involved in the disease progression, further studies will be required to clarify the roles of these genes in the pathogenesis of CML BC.

In this study, by combining our CML transgenic model with retroviral insertional mutagenesis, we demonstrated that overexpression/enhanced kinase activity of BCR/ABL and expression of Notch1ΔC/NICDΔC contribute to CML BC. Our results provide insights in the molecular mechanism(s) responsible for the disease evolution of human CML and find this transgenic system to be a valuable tool to identify genes whose altered expression and/or structural change cooperate with p210BCR/ABL to induce BC.

Materials and Methods

Transgenic mice and retrovirus infection

p210BCR/ABL Tg were generated as described (Honda *et al.*, 1998). *lck/Notch1ΔC* Tg were generated as follows; A fragment containing the *PEST* domain mouse *Notch1* cDNA (a kind gift from Dr. Chiba in Tokyo University) was replaced by a fragment released from BstYI5'/6-4 (an iPCR product of MMLV-6, where the retrovirus was integrated in the last exon of *Notch1* gene, see supplemental Table 1), which created cDNA lacking the C-terminal *PEST* domain (*Notch1ΔC*). *Flag-HA* (*FH*) sequences were added to the 5'end of *Notch1ΔC*, which was subcloned into a transgenic cassette possessing the *lck* promoter (Abraham *et al.*, 1991). A fragment containing the *lck* promoter, *FH, Notch1ΔC*, and a part of *human growth hormone* (*hGH*) gene was excised and microinjected into pronuclei of C57BL/6N mice. All the mice were kept according to the guidelines of the Institute of Laboratory Animal Science, Hiroshima University.

Preparation and infection of retrovirus were performed as described (Wolff *et al.*, 2003a; Wolff *et al.*, 2003b). In brief, newborn mice were intraperitoneally inoculated with 100 μl of virus solution containing approximately $1X10^5$ virus particles.

Pathological analysis

Autopsies were performed on dead or moribund animals. Smears and stamp specimens of leukemic tissues were stained with Wright-Giemsa (WG). Tissues were fixed in 10% buffered formaldehyde and subjected to light microscopic examination. All the organs were grossly examined and representative slices were prepared for hematoxylin-eosin (HE) staining.

Flowcytometric analysis

Leukemic cells were stained with fluorescein isothiocyanate (FITC)-conjugated or

phycoerythrin (PE)-conjugated monoclonal antibodies, including anti-Thy-1.2, anti-B220, anti-Gr.1, and anti-Mac1 (Pharmingen, San Diego, CA) and were analyzed on a FACS Calibur (Becton Dickinson, Sunnyvale, CA).

Identification of retroviral integration sites

Genomic DNA was digested with BstYI (New England Biolabs, Inc., Beverly, MA), self-ligated, and subjected to the inverse PCR as described elsewhere (Yamashita *et al.*, 2005). The position mapping on the mouse chromosome was done by BLAT searching using the UCSC Genome Bioinformatics database (http://genome.ucsc.edu) and the definition of a common integration site (CIS) was the same in the retroviral-tagged cancer gene database (RTCGD) (http://rtcgd.abcc.ncifcrf.gov/)(Akagi *et al.*, 2004).

Southern and Northern blot

Genomic DNA was digested with appropriate restriction enzymes, separated in 0.8% agarose gel, blotted to a nylon membrane, and hybridized with a ^{32}P-dCTP labeled probe. Total RNA was extracted using TRIzol (Invitrogen, California, CA), separated in 1.2% formaldehyde gel, blotted to a nylon membrane, and hybridized with a ^{32}P-dCTP labeled probe.

Western blot, immunoprecipitation, and *in vitro* kinase assay

Tissues were lysed in 1% Triton buffer as described (Honda *et al.*, 1995). For Western blot, proteins were separated by SDS-PAGE, transferred to a nitrocellulose membrane, incubated with an appropriate antibody (1:500 for anti-Notch1 monoclonal antibody, mN1A (Santa Cruz, California, CA), 1:1000 for anti-Notch1 polyclonal antibody, Val1477 (Cell Signaling Technology, Danvers, MA), 1:1000 for anti-Flag monoclonal antibody, M2 (Sigma-Aldrich, St Louis, MO), 1:500 for anti-ABL

polyclonal antibody, Ab1 (Oncogene Science, Cambridge, MA), 1:2000 for anti-phosphotyrosine monoclonal antibody, 4G10 (a kind gift from Dr. Sakai in National Cancer Center), and 1:500 for anti-Stat5 polyclonal antibody, C-17 (Santa Cruz, California, CA)), and developed with the enhanced chemiluminescence (ECL) system. For immunoprecipitation, proteins were incubated with 1:200 diluted an anti-Stat5 antibody and immunoprecipitated proteins were blotted with 4G10 (1:2000) or with the same antibody (1:500). For *in vitro* kinase assay, protein was incubated with 1:200 diluted an anti-ABL antibody and immunoprecipitated proteins were subjected to the assay as described (Honda *et al.*, 1995).

Acknowledgements

We thank Yuki Sakai, Kayoko Hashimoto, Yuko Tsukawaki for mouse care and technical assistance and thank Shigeru Chiba and Ryuichi Sakai for providing us with mouse *Notch1* cDNA and anti-phosphotyrosine antibody. This work was supported by a Grant-in-Aid from the Ministry of Education, Science and Culture of Japan, a Grant-in-Aid for Cancer Research from the Ministry of Health, Labour and Welfare of Japan (13-2), Research Grant of the Princess Takamatsu Cancer Research Fund, Mitsubishi Pharma Research Foundation, YASUDA Medical Research Foundation, a Grant-in-Aid of The Japan Medical Association, and Japan Leukaemia Research Fund.

Supplemental information is available at Oncogene's website.

References

Abraham KM, Levin SD, Marth JD, Forbush KA, Perlmutter RM. (1991). Thymic tumorigenesis induced by overexpression of p56lck. *Proc Natl Acad Sci USA*, **88**: 3977-3981.

Akagi K, Suzuki T, Stephens RM, Jenkins NA, Copeland NG. (2004). RTCGD: retroviral tagged cancer gene database. *Nucleic Acids Res*, **32 (Database issue)**: D523-527.

Bray SJ. (2006). Notch signalling: a simple pathway becomes complex. *Nat Rev Mol Cell Biol*, **7**: 678-689.

Calabretta B, Perrotti D. (2004). The biology of CML blast crisis. *Blood*, **103**: 4010-4022.

Deininger MWN, Goldman JM, Melo JV. (2000). The molecular biology of chronic myeloid leukemia. *Blood*, **96**: 3343-3356.

Ellisen LW, Bird J, West DC, Soreng AL, Reynolds TC, Smith SD, *et al.* (1991). TAN-1, the human homolog of the Drosophila notch gene, is broken by chromosomal translocations in T lymphoblastic neoplasms. *Cell*, **66**: 649-661.

Grabher C, von Boehmer H, Look AT. (2006). Notch 1 activation in the molecular pathogenesis of T-cell acute lymphoblastic leukaemia. *Nat Rev Cancer*, **6**: 347-359.

Honda H, Fujii T, Takatoku M, Mano H, Witte ON, Yazaki Y, *et al.* (1995). Expression of $p210^{bcr/abl}$ by metallothionein promoter induced T-cell leukemia in transgenic mice. *Blood*, **85**: 2853-2861.

Honda H, Oda H, Suzuki T, Takahashi T, Witte ON, Ozawa K, *et al.* (1998). Development of acute lymphoblastic leukemia and myeloproliferative disorder in transgenic mice expressing $p210^{bcr/abl}$: a novel transgenic model for human Ph1-positive leukemias. *Blood*, **91**: 2067-2075.

Honda H, Ozawa K, Yazaki Y, Hirai H. (1997). Identification of PU.1 and Sp1 as

essential transcriptional factors for the promoter activity of mouse *tec* gene. *Biochem Biophys Res Commun*, **234**: 376-381.

Honda H, Ushijima T, Wakazono K, Oda H, Tanaka Y, Aizawa S-i, *et al.* (2000). Acquired loss of p53 induces blastic transformation in $p210^{bcr/abl}$-expressing hematopoietic cells: a transgenic study for blast crisis of human CML. *Blood*, **95**: 1144-1150.

Huettner CS, Zhang P, Van Etten RA, Tenen DG. (2000). Reversibility of acute B-cell leukaemia induced by BCR-ABL1. *Nat Genet*, **24**: 57-60.

Huettner CS, Koschmieder S, Iwasaki H, Iwasaki-Arai J, Radomska HS, Akashi K, *et al.* (2003). Inducible expression of BCR/ABL using human CD34 regulatory elements results in a megakaryocytic myeloproliferative syndrome. *Blood*, **102**: 3363-3370.

Ilagan MX and Kopan R. (2007). SnapShot: notch signaling pathway. *Cell*, **128**: 1246

Jonkers J, Berns A. (1996). Retroviral insertional mutagenesis as a strategy to identify cancer genes. *Biochem Biophys Acta*, **1287**: 29-57.

Kamakura S, Oishi K, Yoshimatsu T, Nakafuku M, Masuyama N, Gotoh Y. (2004). Hes binding to STAT3 mediates crosstalk between Notch and JAK-STAT signalling. *Nat Cell Biol*, **6**: 547-554.

Koschmieder S, Gottgens B, Zhang P, Iwasaki-Arai J, Akashi K, Kutok JL, *et al.* (2005). Inducible chronic phase of myeloid leukemia with expansion of hematopoietic stem cells in a transgenic model of BCR-ABL leukemogenesis. *Blood*, **105**: 324-334.

Li S, Ilaria RLJ, Million RP, Daley GQ, Van Etten RA. (1999). The P190, P210, and P230 forms of the BCR/ABL oncogene induce a similar chronic myeloid leukemia-like syndrome in mice but have different lymphoid leukemogenic activity. *J Exp Med*, **189**: 1399-1342.

Lin YW, Nichols RA, Letterio JJ, Aplan PD. (2006). Notch1 mutations are important for

leukemic transformation in murine models of precursor-T leukemia/lymphoma. *Blood*, **107**: 2540-2543.

Mikkers H, Berns A. (2003). Retroviral insertional mutagenesis: tagging cancer pathways. *Adv Cancer Res*, **88**: 53-99.

Monsalve E, Pérez MA, Rubio A, Ruiz-Hidalgo MJ, Baladrón V, García-Ramírez JJ, *et al*. (2006). Notch-1 up-regulation and signaling following macrophage activation modulates gene expression patterns known to affect antigen-presenting capacity and cytotoxic activity. *J Immunol*, **176**: 5362-5373.

Nakamura T. (2005). Retroviral insertional mutagenesis identifies oncogene cooperation. *Cancer Sci*, **96**: 7-12.

Niki M, Cristofano DA, Zhao M, Honda H, Hirai H, Aelst VL, *et al.* (2004). Role of Dok-1 and Dok-2 in leukemia suppression. *J Exp Med*, **200**: 1689-1695.

O'Nei lJ, Calvo J, McKenna K, Krishnamoorthy V, Aster JC, Bassing CH, *et al.* (2006). Activating Notch1 mutations in mouse models of T-ALL. *Blood*, **107**: 781-785.

Pane F, Intrieri M, Quintarelli C, Izzo B, Muccioli GC, Salvatore F. (2002). Activating Notch1 mutations in mouse models of T-ALL. *Oncogene*, **21**: 8652-8667.

Pear WS, Miller JP, Xu L, Pui JC, Soffer B, Quackenbush RC, *et al.* (1998). Efficient and rapid induction of a chronic myelogenous leukemia-like myeloproliferative disease in mice receiving P210bcr/abl-transduced bone marrow. *Blood*, **92**: 3780-3792.

Ren R. (2005). Mechanisms of BCR-ABL in the pathogenesis of chronic myelogenous leukaemia. *Nat Rev Cancer*, **5**: 172-183.

Rowley JD. (1973). A new consistent chromosomal abnormality in chronic myelogenous leukemia identified by quinacrine fluorescence and Giemsa staining. *Nature*, **243**: 290-293.

Scherr M, Chaturvedi A, Battmer K, Dallmann I, Schultheis B, Ganser A *et al.* (2006). Enhanced sensitivity to inhibition of SHP2, STAT5, and Gab2 expression in

chronic myeloid leukemia (CML). *Blood*, **107**: 3279-3287.

Shore SK, La Cava M, Yendapalli S, Reddy EP. (1994). Structural alterations in the carboxyl-terminal domain of the BCRABL gene product activate its fibroblastic transforming potential. *J Biol Chem*, **269**: 5413-5419.

Shuai K, Halpern J, ten Hoeve J, Rao X, Sawyers CL. (1996). Constitutive activation of STAT5 by the BCR-ABL oncogene in chronic myelogenous leukemia. *Oncogene*, **13**: 247-254.

Voncken JW, Kaartinen V, Pattengale PK, Germeraad WTV, Groffen J, Heisterkamp N. (1995). *BCR/ABL* p210 and p190 cause distinct leukemia in transgenic mice. *Blood*, **86**: 4603-4611.

Weng AP, Ferrando AA, Lee W, Morris JP 4th, Silverman LB, Sanchez-Irizarry C, *et al*. (2004). Activating mutations of NOTCH1 in human T cell acute lymphoblastic leukemia. *Science*, **306**: 269-271.

Wolff L, Garin MT, Koller R, Bies J, Liao W, Malumbres M, *et al*. (2003a). Hypermethylation of the Ink4b locus in murine myeloid leukemia and increased susceptibility to leukemia in p15(Ink4b)-deficient mice. *Oncogene*, **22**: 9265-9274.

Wolff L, Koller R, Hu X, Anver MR. (2003b). A Moloney murine leukemia virus-based retrovirus with 4070A long terminal repeat sequences induces a high incidence of myeloid as well as lymphoid neoplasms. *J Virol*, **77**: 4965-4971.

Yamashita N, Osato M, Huang L, Yanagida M, Kogan SC, Iwasaki M, *et al*. (2005). Haploinsufficiency of Runx1/AML1 promotes myeloid features and leukaemogenesis in BXH2 mice. *Br J Haematol*, **131**: 495-507.

Ye D, Wolff N, Li L, Zhang S, Ilaria RLJ. (2006). STAT5 signaling is required for the efficient induction and maintenance of CML in mice. *Blood*, **107**: 4917-4925.

Zhang X, Ren R. (1998). Bcr-Abl efficiently induces a myeloproliferative disease and production of excess interleukin-3 and granulocyte-macrophage

colony-stimulating factor in mice: a novel model for chronic myelogenous leukemia. *Blood*, **92**: 3829-3840.

Title and legends for figures

Figure 1. (A) Kaplan-Meyer survival curves of MMLV-injected p210BCR/ABL Tg (p210BCR/ABL/MMLV, solid line) and WT (WT/MMLV, dotted line). The death points of p210BCR/ABL/MMLV (MMLV-1~10) are indicated. (B) Kaplan-Meyer survival curves of MOL4070LTR-injected p210BCR/ABL Tg (p210BCR/ABL/MOL4070, solid line) and WT (WT/MOL4070, dotted line). The death points of 6 p210BCR/ABL/MOL4070 (MOL4070-1~6) are indicated and disease phenotypes of the mice are shown in the parentheses (B, B-cell leukemia and T, T-cell leukemia).

Figure 2. (A) Pathological analysis of the leukemic mice. Results of WG-stained peripheral blood smears (PB) and HE-stained lymphnode (LN) and liver slices for T-cell leukemia (MMLV-2) and B-cell leukemia (MOL4070-1) are shown. In both cases, blast cells proliferated in the PB, destructed the basal structure in the LN, and infiltrated around the vessel and in the sinusoids in the liver. (B) Results of a flow cytometric analysis of mice that developed B-cell or T-cell leukemia. Blast cells of MMLV-2 were positive for Thy1.2, whereas those of MOL4070-1 were positive for CD19, indicating that they were of T- and B-lymphoid origins, respectively.

Figure 3 (A) Schematic illustration of the transgene identified as a CIS in 2 B-ALL cases (MOL4070-1 and MOL4070-2) and the resultant gene products. In the transgene, virus integration sites are indicated by vertical arrows, and in the gene products, virus-derived region is underlined and altered nucleic acid and amino acid sequences are shown in lowercase (SH3; src homology 3, SH2; src homology 2, KD; kinase domain, NLS/DBD; nuclear localization signal/DNA binding domain, ABD; actin-binding domain). (B) Southern blot for gene rearrangement. Five μg genomic DNAs extracted from a spleen of a control transgenic mouse (C) and tumor tissues of MOL4070-1 and MOL4070-2 were digested with restriction enzymes and probed with a

part of mouse *TEC* promoter (left panel) or a part of *ABL*-coding region (right panel). Rearranged bands are indicated by arrowheads. (C) Northern blot for *BCR/ABL* mRNA. Twenty μg total RNAs of a control transgenic spleen (C), tumors of MOL4070-1 and MOL4070-2, and tumors of MOL4070-3~MOL4070-5 in which retrovirus was not integrated in the transgene were probed with *BCR/ABL* cDNA. Overexpressed *p210BCR/ABL* mRNA in MOL4070-1 is indicated by an arrowhead. *β-actin* hybridization is shown as an internal control. (D) *In vitro* kinase assay for BCR/ABL-mediated kinase activity. One mg proteins extracted from the same tissues as (C) were incubated with an anti-ABL antibody, and immunoprecipitated proteins were subjected to the *in vitro* kinase assay. Phosphorylated p210BCR/ABL in MOL4070-1 and truncated BCR/ABL in MOL4070-2 are indicated by an arrowhead and by an arrow, respectively.

Figure 4 (A) Schematic illustration of *Notch1* gene identified as a CIS found in 2 T-ALL cases (MMLV-1 and MMLV-6) and the resultant gene products. In *Notch1* gene, virus integration sites are indicated by vertical arrows, and in the gene products, virus-derived region is underlined, and altered nucleic acid and amino acid sequences are shown in lowercase (LIN; LIN12 repeats, TM; transmembrane, RAM; RAM domain, ANK; ankyrin repeats, TAD; transactivation domain, PEST; polypeptide enriched in proline, glutamate, serine, and threonine). (B) Southern blot for gene rearrangement. Five μg genomic DNAs extracted from a control transgenic mouse thymus (C) and tumor tissues of MMLV-1 and MMLV-6 were digested with restriction enzymes and probed with an adjacent genomic fragment. Rearranged bands are indicated by arrowheads. (C) Northern blot for *Notch1* mRNA. Twenty μg total RNAs of a control transgenic spleen (C), tumors of MMLV-1 and MMLV-6, and tumors of MMLV-3~MMLV-5 in which retrovirus was not integrated in *Notch1* were probed with *Notch1* cDNA. Overexpressed *Notch1* mRNA in MMLV-1 and truncated *Notch1* mRNA in MMLV-6 are indicated by

an arrowhead and by an arrow, respectively. *β-actin* hybridization is shown as an internal control. (D) Western blot for Notch1. Thirty μg proteins extracted from the same tissues as (C) were blotted with an anti-Notch1 antibody, mN1A (upper panel) or Val1477 (lower panel). In the upper panel, the positions of Notch1 and its cleaved product, NTM, are shown on the right, the overexpressed Notch1 and enhanced expression of NTM in MMLV-1 are indicated by black and white triangles, and expression of truncated Notch1 (Notch1ΔC) and stable expression of truncated NTM (NTMΔC) in MMLV-6 are indicated by arrows. In the lower panel, expression of NICDΔC is indicated by an arrow. Protein markers are shown on the left.

Figure 5 (A) Schematic illustration of the transgene for *lck/Notch1ΔC* Tg. A DNA fragment containing the *lck* promoter, *Flag/HA* (*FH*) tag, *Notch1ΔC* cDNA, and a part of *human growth hormone gene* (*hGH*) was used to generate *lck/Notch1ΔC* Tg. (B) Kaplan-Meyer survival curves of *p210BCR/ABL* Tg, *lck/Notch1ΔC* Tg, and double Tg (*p210BCR/ABL*X*lck/Notch1ΔC* Tg) are plotted as thin solid, thick dotted, and thick solid lines, respectively. During the observation period, a half of double Tg died of T-ALL, whereas none of Tg for *p210BCR/ABL* or *lck/Notch1ΔC* alone developed leukemia. (C) Western blot for expression of Notch1ΔC/NTMΔC and NICDΔC, and p210BCR/ABL in control transgenic thymuses and in the tumor tissues. Thirty μg proteins extracted from a *p210BCR/ABL* Tg thymus (C1), an *lck/Notch1ΔC* Tg thymus (C2), and tumor tissues of double Tg (No. 1~4) were blotted with anti-Notch1 antibodies (upper panel with mN1A and middle panel with Val1477) or an anti-ABL antibody (lower panel). In the upper panel, the positions of Notch1/NTM and Notch1ΔC/NTMΔC are indicated by arrows and in the middle panel, the expression of NICDΔC is indicated by an arrow. In the lower panel, the expression of p210BCR/ABL is indicated by an arrow. Protein markers are shown on the left. (D) Western blot for tyrosine-phosphorylated proteins in the tumor tissues. In the upper panel, thirty μg of

proteins extracted from the same tissues as (C) were blotted with an anti-phosphotyrosine (PTyr) antibody. Two major tyrosine-phosphorylated bands are indicated by an arrow and an arrowhead. In the lower panels, one mg proteins were incubated with an anti-Stat5 antibody and immunoprecipitated proteins were blotted with an anti-PTyr or an anti-Stat5 antibody. Protein markers are shown on the left.

Fig.1

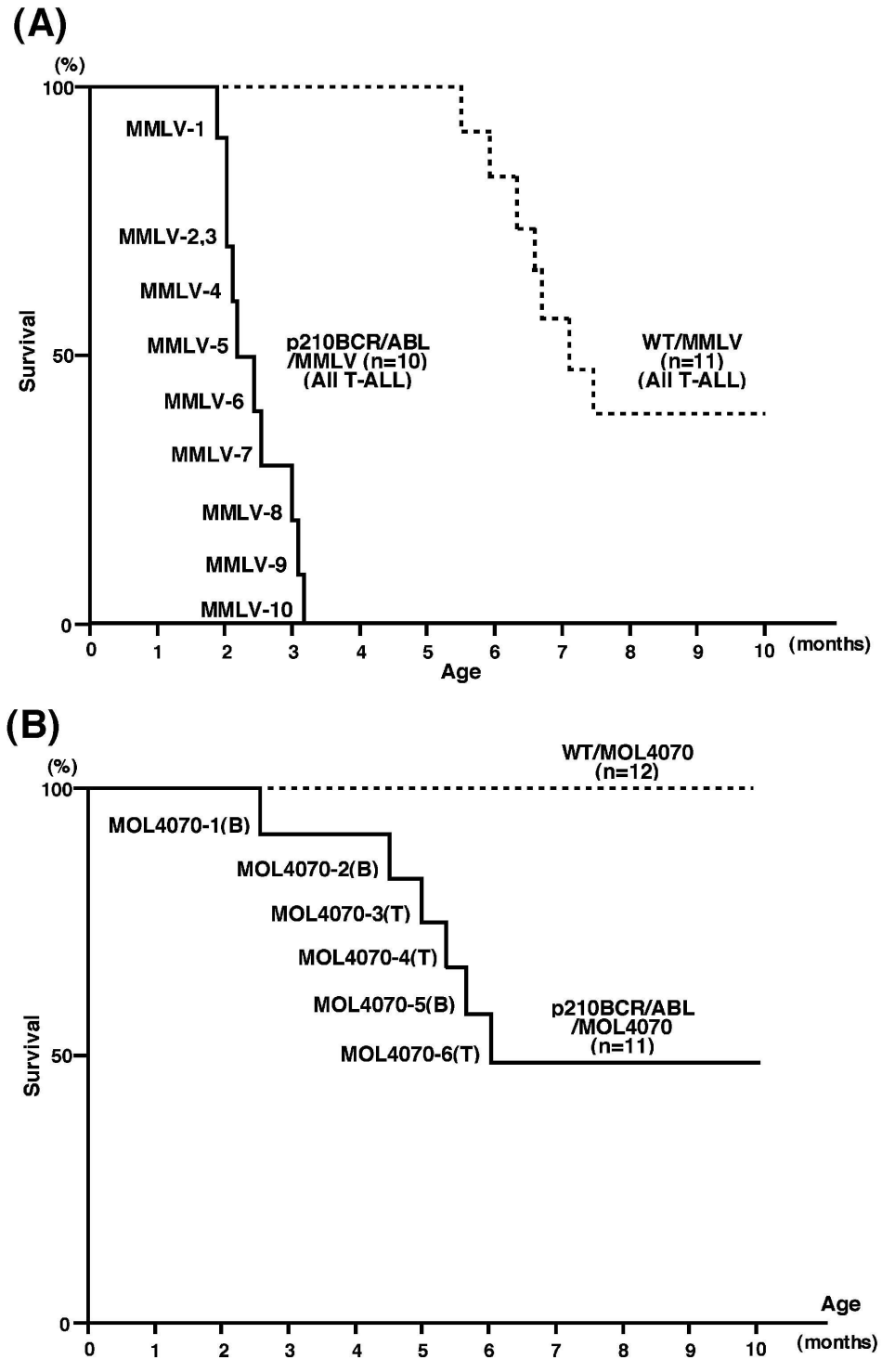

Figure 1 Mizuno T. *et al.*

Fig.2

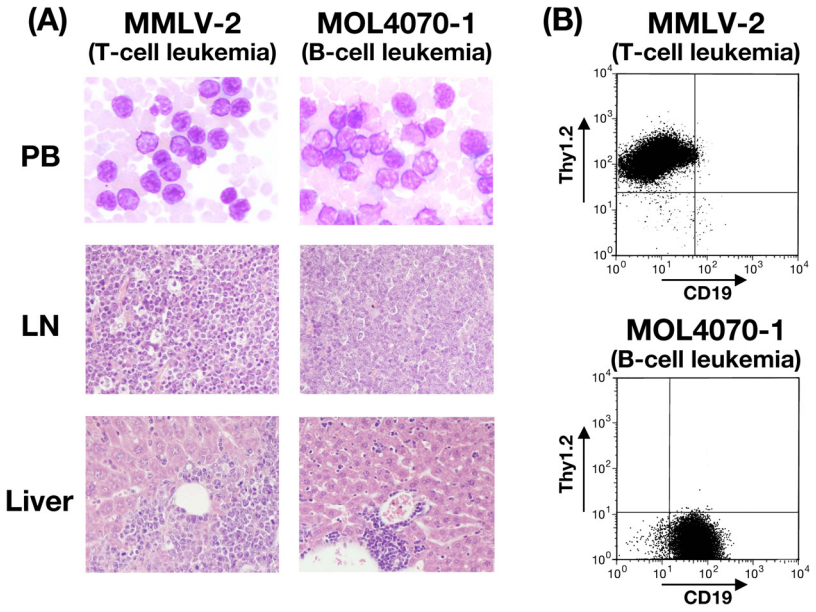

Figure 2 Mizuno T. *et al.*

Fig.3

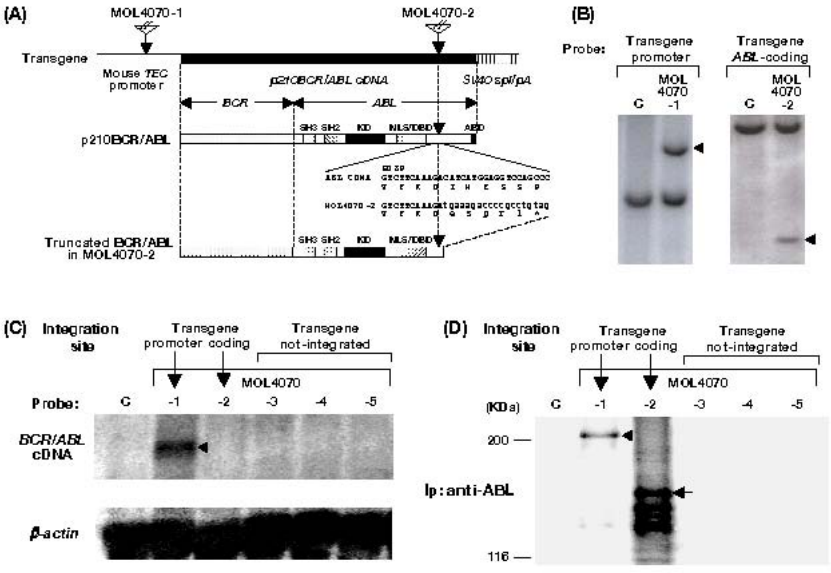

Figure 3 Mizuno T. *et al.*

Fig.4

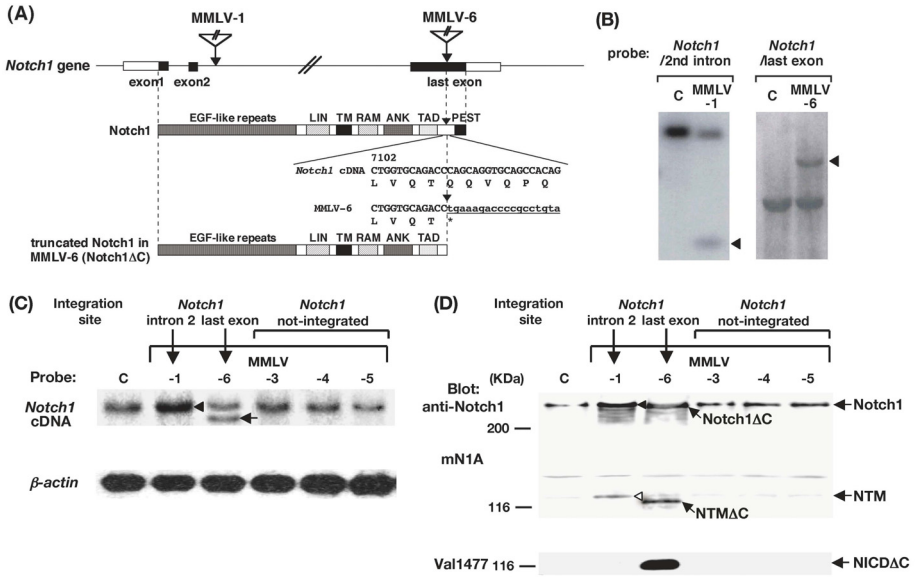

Figure 4 Mizuno T. *et al.*

Fig.5

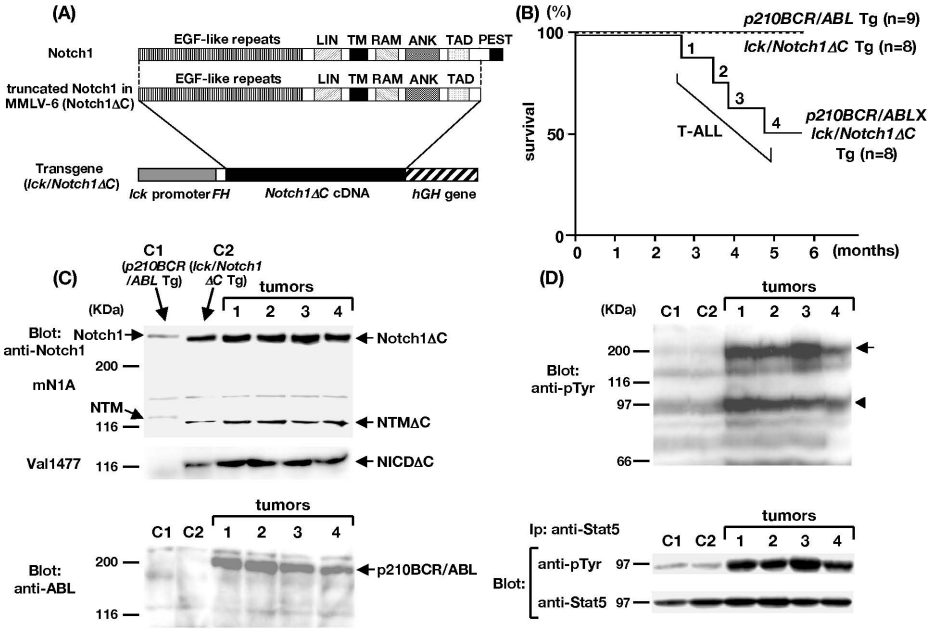

Figure 5 Mizuno T. *et al.*

Table 1

Table 1. Characteristics of leukemias in p210BCR/ABL/MMLV

Mouse No.	Age at* disease (month)	PB parameters† WBC ($X10^3/\mu L$)	Hb (g/dL)	PLT ($X10^4/\mu L$)	Macroscopic‡ tumor sites	Surface markers	Diagnosis
M-1	1.8 d	N.D.	N.D.	N.D.	Thy, Spl, LN	N.D.	T-cell leukemia, s/o
M-2	2.0	21.5	13.8	21.1	Thy, Spl	Thy1.2(+), B220(-)	T-cell leukemia
M-3	2.0	89.0	14.9	33.8	Thy, Spl, LN	Thy1.2(+), B220(-)	T-cell leukemia
M-4	2.1	18.5	14.4	49.2	Thy, Spl	Thy1.2(+), B220(-)	T-cell leukemia
M-5	2.2	10.5	14.6	37.8	Thy, Spl	Thy1.2(+), B220(-)	T-cell leukemia
M-6	2.4	14.5	13.0	36.5	Thy, Spl, LN	Thy1.2(+), B220(-)	T-cell leukemia
M-7	2.5	3.4	15.3	41.1	Thy, Spl	Thy1.2(+), B220(-)	T-cell leukemia
M-8	3.0	11.8	13.7	54.6	Thy, Spl	Thy1.2(+), B220(-)	T-cell leukemia
M-9	3.1	30.9	13.5	27.8	Thy, Spl, LN	Thy1.2(+), B220(-)	T-cell leukemia
M-10	3.2	7.1	13.2	51.5	Thy, Spl	Thy1.2(+), B220(-)	T-cell leukemia

* d, found dead
† N.D., not done
‡ Thy, thymus; Spl, spleen, LN, lymphnode

Table 2

Table 2. Characteristics of leukemias in p210BCR/ABL/MOL4070

Mouse No.	Age at disease (month)	PB parameters WBC ($X10^3/\mu L$)	Hb (g/dL)	PLT ($X10^4/\mu L$)	Macroscopic‡ tumor sites	Surface markers	Diagnosis
4070-1	3.1	62.4	9.2	58.8	Tumor on shouler, Spl	Thy1.2(-), B220(+)	B-cell leukemia
4070-2	4.5	51.9	9.7	60.2	Spl, LN	Thy1.2(-), B220(+)	B-cell leukemia
4070-3	5.0	8.9	12.0	44.9	Thy, Spl	Thy1.2(+), B220(-)	T-cell leukemia
4070-4	5.3	10.5	14.4	49.2	Thy, Spl	Thy1.2(+), B220(-)	T-cell leukemia
4070-5	5.6	41.0	6.6	13.0	Spl, LN	Thy1.2(-), B220(+)	B-cell leukemia
4070-6	6.0	32.5	8.0	21.6	Thy, Spl, LN	Thy1.2(+), B220(-)	T-cell leukemia

‡ Thy, thymus; Spl, spleen, LN, lymphnode

Supplemental Figure 1

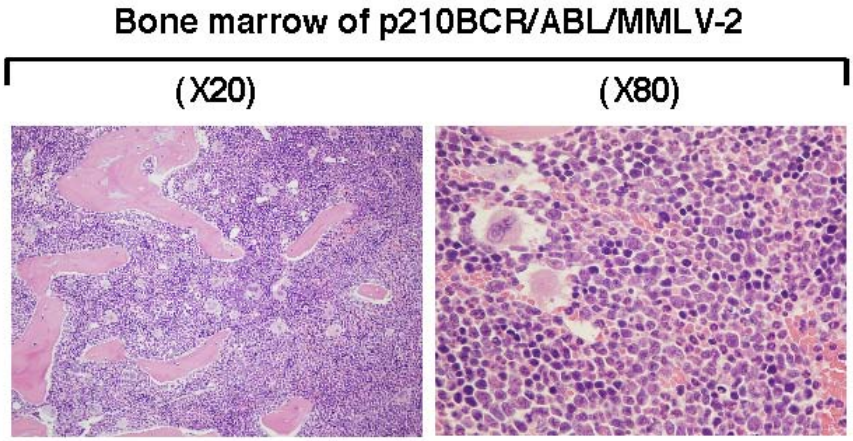

Supplemental figure 1. Bone marrow picture of p210BCR/ABL/MMLV-2 at 2 months of age, when the mouse developed T-ALL. In the lower magnification (X20, left), the bone marrow is hypercellular with predominance of myeloid cells. Increase in megakaryocytes is also observed. In the higher magnification (X80, right), proliferation of myeloid cells with differentiation is evident. These findings are a characteristic feature of CML CP.

Supplemental Figure 1 Mizuno T. *et al.*

Supplemental Figure 2

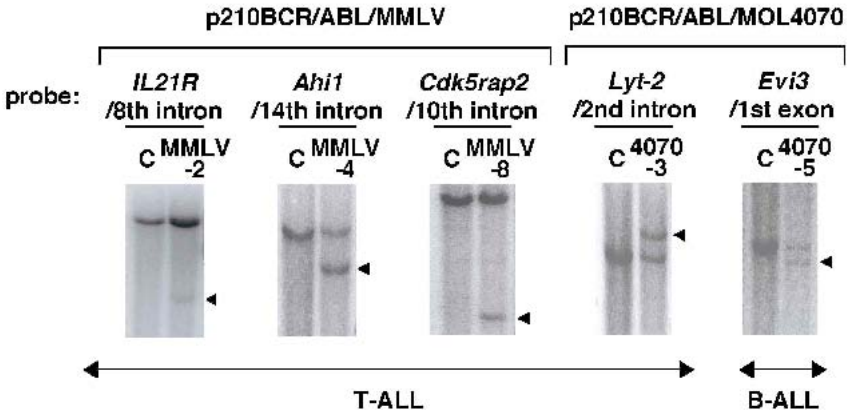

Supplemental figure 2. Results of Southern blots that showed rearranged bands in genes of *IL21 receptor* (*IL21R*), *Ahi1*, *Cdk5rap2*, and *Lyt-2* for T-ALL and *Evi3* for B-ALL. Rearranged bands are indicated by arrowheads.

Supplemental Figure 2 Mizuno T. *et al.*

Supplemental Figure 3

Supplemental Table 1. Genes identified by iPCR in p210BCR/ABL/MMLV leukemic samples

Mouse No.	PCR fragment No.	Gene name	Chromosome position	Integration site	Description
MMLV-1	BstYI5'/1-1	Gata3	2qA1	3' downstream (~70kb)	Trans-acting T-cell specific transcription factor GATA-3
	BstYI3'/1-1	***Notch1**	**2qA3**	**2nd intron**	**Notch gene homolog 1 (Notch 1)**
	BstYI3'/1-2	Atp5f1	3qF2.2	5' upstream (~10kb)	Mitochondrial ATP synthase chain
	BstYI5'/1-2	Eif3s2	4qD2.2	5' upstream (~2kb)	Eukaryotic translation initiation factor 3
MMLV-2	BstYI5'/2-1	Mod1	9qE3.1	5th intron	Similar to malic enzyme, supernatant
	BstYI3'/2-1	**Il21r**	**7qF3**	**8th intron**	**Interleukin 21 receptor precursor**
	BstYI3'/2-2	Traf1	2qB	1st intron	TNF receptor associated factor 1
	BstYI3'/2-3	Evl	12qF1	5th intron	Ena/vasodilator stimulated phosphoprotein-like protein
MMLV-3	BstYI5'/3-1	Tbc1d16	11qE2	6th intron	TBC1 domain family member 16
	BstYI5'/3-2	Edem1	6qE2	3rd intron	EDEM protein homolog
	BstYI3'/3-1	Ptpn1	2qH3	5' upstream (~20kb)	Protein-tyrosine phosphatase 1B
MMLV-4	BstYI3'/4-1	BC043727	3qF2.3	1st intron	2010308M01Rik protein
	BstYI3'/4-2	**Ahi**	**10qA3**	**14th intron**	**Ahi/Jouberin (Abelson helper integration site 1 protein)**
MMLV-5	BstYI5'/5-1	Myb(-)	10qA3	5' upstream (~20kb)	Myb proto-oncogene protein
	BstYI5'/5-2	Zfp239	6qF1	3' downstream (~20kb)	Zinc finger protein 239
	BstYI5'/5-3	Tspan5	3qH1	2nd intron	Tetraspanin 5
	BstYI3'/5-1	Vegfa	17qB3	5' upstream (~2kb)	Vascular endothelial GFA precursor/VEGF
	BstYI3'/5-2	Sema4a	3qF1	2nd intron	Semaphorin 4A precursos
MMLV-6	BstYI5'/6-1	Gapd	6qF3	2nd intron	Glyceraldehyde-3-phosphate dehydrogenase
	BstYI5'/6-2	Skb1	14qC1	2nd intron	Protein arginine N-methyltransferase/JBP1
	BstYI5'/6-3	St8sia1	6qG3	1st intron	Alpha 2,8-sialyltransferase
	BstYI5'/6-4	***Notch1**	**2qA3**	**last exon (disrupt coding)**	**Notch gene homolog 1 (Notch 1)**
MMLV-7	BstYI5'/7-1	Mpp1	XqA7.3	1st intron	Erythrocyte membrane protein 55/PEMP
	BstYI5'/7-2	Cdk6(-)	5qA1	5' upstream (~1kb)	Cell division protien kinase 6/PLSTIRE
	BstYI5'/7-3	Glipr2	4qB1	4th intron	Golgi-associated plant pathogenesis-related protein 1
	BstYI3'/7-1	Fstl3	10qC1	last exon	Follistatin-like 3
	BstYI3'/7-2	Tcl7(-)	11qB1.3	1st intron	T-cell specific transcription factor 7/TCF-1
MMLV-8	BstYI5'/8-1	Tle3(-)	9qB	3' downstream (~20kb)	Transducin-like enhancer of split 3
	BstYI3'/8-1	LrrC1	9qE1	2nd intron	Leucine rich repeat protein 1
	BstYI3'/8-2	Piwil2	14qD1	1st intron	Piwi like homolog 2/Mili
MMLV-9	BstYI5'/9-1	Tesc	5qF	1st intron	Tescalcin
	BstYI5'/9-2	**Cdk5rap2**	**4qC1-qC2**	**11th intron**	**Cdk5 regulatory subunit associated protein 2**
	BstYI3'/9-1	Man1c1	4qD3	1st intron	Mannosidase alpha class 1C
MMLV-10	BstYI5'/10-1	Mef2b	8qB3.3	1st intron	Myocyte specific enhancer factor 2B
	BstYI5'/10-2	Esf4	8qD3	5' upstream (~2kb)	E2F transcription factor 4
	BstYI5'/10-3	Nkx2-2	2qG2	5' upstream (~1kb)	Nk2 transcription factor related
	BstYI3'/10-1	Pp11r(-)	15qF1	5' upstream (~10kb)	placental protein 11 related/Tcl30
	BstYI3'/10-2	Gfi1 (-)	5qE5	3' downstream (~20kb)	Growth factor independent 1

Genes in bold-face are major integration sites demonstrated by Southern blots and asterisks indicate common integration sites (CISs).
(-) after gene namges indicates that we performed Southern blots but could not detect rearranged bands.

Supplemental Table 1 Mizuno T. *et al.*